



**CORNELL AERONAUTICAL LABORATORY, INC.**

OF CORNELL UNIVERSITY

P. O. BOX 235 • BUFFALO, NEW YORK • 14221

TELEPHONE 716-632-7800

AD743121

SEMIANNUAL TECHNICAL REPORT  
For Period 1 November 1971 to 1 May 1972

CAL Report No. AI-3107-A-2

EXPERIMENTAL STUDIES OF PHOTOIONIZATION PROCESSES IN AIR

Contract No.: N00014-71-C-0387

Program Code No.: 000001E20K21

Principal Investigator: Dr. Walter H. Wurster (716)632-7500 ext. 501

Scientific Officer: Director, Physics Program, Physical Sciences Div.  
Office of Naval Research  
Department of the Navy  
800 N. Quincy Street  
Arlington, Virginia 22217

**DISTRIBUTION STATEMENT A**  
Approved for public release;  
Distribution Unlimited

Effective Date of Contract: May 1, 1971

Amount of Contract: \$45,000

DDC  
REGISTERED  
JUN 8 1972  
C

The views and conclusions contained in this document are those of the authors and should not be interpreted as necessarily representing the official policies, either expressed or implied, of the Advanced Research Projects Agency or the U.S. Government.

Reproduced by  
**NATIONAL TECHNICAL  
INFORMATION SERVICE**  
Springfield, Va. 22151

Sponsored by:  
Advanced Research Projects Agency  
ARPA Order No. 1479, Amendment No. 3/3-11-71

SEE AD777777

**BEST  
AVAILABLE COPY**

## DOCUMENT CONTROL DATA - R &amp; D

(Security classification of title, body of abstract and indexing annotation must be entered when the overall report is classified)

1 ORIGINATING ACTIVITY (Corporate author) Cornell Aeronautical Laboratory, Inc. 4455 Genesee St. Buffalo, New York 14221		2a. REPORT SECURITY CLASSIFICATION Unclassified	
		2b. GROUP None	
3 REPORT TITLE EXPERIMENTAL STUDIES OF PHOTOIONIZATION PROCESSES IN AIR			
4 DESCRIPTIVE NOTES (Type of report and inclusive dates) Semiannual Technical Report - Performance Period 11/1/71 - 5/1/72			
5 AUTHOR(S) (First name, middle initial, last name) Walter H. Wurster			
6 REPORT DATE May 1972	7a. TOTAL NO. OF PAGES 35	7b. NO. OF REFS 13	
8a. CONTRACT OR GRANT NO N00014-71-C-0387	8a. ORIGINATOR'S REPORT NUMBER(S) AI-3107-A-2		
b. PROJECT NO	8b. OTHER REPORT NO(S) (Any other reports that may be assigned this report)		
c. Program Code No. 000001E20K21			
d.			
10 DISTRIBUTION STATEMENT			
11 SUPPLEMENTARY NOTES		12. SPONSORING MILITARY ACTIVITY Advanced Research Projects Agency Office of Naval Research	

## 13 ABSTRACT

An experimental study is described whose objectives is to assess the role of NO in the nonequilibrium vacuum ultraviolet (VUV) radiation from shock-heated air. The experiment utilizes a splitter-plate shock tube technique wherein the VUV radiation behind a reflected shock is used as a light source to measure the absorption by gases processed only by the incident shock wave. In addition, nonequilibrium radiation profiles behind strong incident shock waves are also measured to aid in the identification of the relevant excitation processes.

This report describes the apparatus, discusses the results of calculations needed to establish testing parameters, and presents the experimental measurements to date.

## TABLE OF CONTENTS

	PAGE
I. INTRODUCTION	1
II. RESEARCH PROGRAM	2
II. 1 Vacuum Ultraviolet Radiation-Measurements	2
II. 1. 1 Experiment Description and Definition	2
II. 1. 2 Experimental Results	6
II. 2 Nonequilibrium Radiation Overshoot	10
II. 2. 1 Calculations	10
II. 2. 2 Experimental Results	11
III. CURRENT STATUS AND FUTURE PLANS	13
REFERENCES	14
FIGURES	16

## TECHNICAL REPORT SUMMARY

### Technical Problem:

An experimental program to investigate basic vacuum ultraviolet photoionization processes in air is currently underway at CAL. Particular emphasis is directed toward the interaction of shock-induced nonequilibrium radiation with gaseous species.

### Methodology:

The experimental shock-tube program consists of three tasks;

1. Perform quantitative measurements to determine the contribution of the NO molecule to the nonequilibrium, vacuum ultraviolet emission spectrum from shock-heated air.
2. Obtain quantitative, spectrally resolved measurements of the nonequilibrium, vacuum ultraviolet flux from advancing shock waves to verify previously developed excitation and radiative flux models.
3. Conduct experiments to determine the relative importance of multiple-step vs. one-step photoionization processes in air.

### Technical Results:

Emphasis thus far has been directed toward the first task, that of determining the role of NO in defining the resultant shock-induced vacuum ultraviolet radiative flux. This semi-annual report presents a brief discussion of the problem, a presentation of experiment definition, and the results of the experimental program to date. Calculations have been completed to determine the important experimental parameters such as shock speed and test gas mixture. Based upon these computations, a series of shock-tube experiments have been initiated, utilizing the splitter-plate absorption technique. The initial shock-tube experiments were directed at obtaining

radiation measurements for a variety of test gas mixtures, both with and without the splitter-plate in the reflecting wall of the shock tube. Vacuum ultraviolet data in the wavelength region  $1050 \text{ \AA} \leq \lambda \leq 1650 \text{ \AA}$  has been obtained using the three-channel VUV spectrometer and an LiF window adapter to couple the spectrometer to the shock tube. Mixtures of NO, N<sub>2</sub> and O<sub>2</sub>, and N<sub>2</sub> in neon have been investigated over a range of shock speeds. These measurements have served to bound the experimental operating conditions under which the NO absorption data can be reliably measured.

In addition to the reflected shock data, nonequilibrium overshoot radiation measurements have been obtained behind the incident shock.

#### Comments:

The major emphasis will now be directed toward obtaining VUV measurements in the  $850 \text{ \AA} \leq \lambda \leq 1100 \text{ \AA}$  wavelength interval using the splitter-plate technique, with the test gas mixture and shock speed determined from the LiF window data obtained to date.

## I. INTRODUCTION

The radiative properties of shock heated gases are much different from those measured at standard conditions, and extrapolations to nonequilibrium situations cannot readily be made. Under strong-shock conditions, vibrational and rotational excited states of the molecular species are populated in nonequilibrium distributions, where different temperatures must be assigned to each of the internal energy modes. The calculation of the ionizing radiative flux emerging from a shock-heated gas has been discussed in Ref. 1, and involves a knowledge of the gas dynamics and chemistry of the flow field, the population of the excited states responsible for the radiation, the spectral shape and distribution of the radiation in the wavelength region of interest, and a knowledge of the radiation transfer process, including emission and absorption in the shock-heated gas. Examples of such situations are found in areas of nuclear effects as well as reentry physics. The rate of early fireball growth, for instance, involves the interaction of photons with shocked atmospheric gases.

The tasks addressed in the present research program are based on results obtained in the course of a reentry-related research program in which the photoionization of the ambient atmosphere in front of a blunt reentry body was treated.<sup>(2, 3, 4)</sup> These results were presented in detail in Ref. 1, and will not be discussed here. However, during the course of those experimental studies for  $N_2$  and subsequent computations for air, the question arose as to the contribution of the NO molecule in the determination of the nonequilibrium VUV emissive and absorptive properties of shock-heated air. Based upon available data for cold NO absorption,<sup>(5, 6, 7)</sup> it may be expected that NO will affect the VUV flux intensity, which highlights the need for absorption coefficient data as a function of temperature.

The experimental research program reported herein is designed to provide data pertinent to vacuum ultraviolet photoionization processes in air. To date, the effort has been directed toward the first task, that of determining the role of NO in the spectral distribution of shock-induced VUV radiation.

## II. RESEARCH PROGRAM

### II.1 Vacuum Ultraviolet Radiation Measurements

#### II.1.1 Experiment Description and Definition

A VUV absorption measurement program for the NO molecule, similar in scope to that described in Refs. 1-4 for the N<sub>2</sub> molecule is currently underway. These measurements are obtained using a high-purity shock tube, with two pertinent features for VUV measurements of this type. The first feature of the experimental arrangement is a 3-channel vacuum ultraviolet spectrometer coupled to the shock tube by an explosively-driven plunger unit, which serves as a fast-acting valve-shutter combination. This windowless plunger was developed under a research program in which photoionization cross sections for N, O, and C were obtained<sup>(8, 9, 10)</sup> from emission measurements in the windowless region of the vacuum ultraviolet ( $\lambda < 1050 \text{ \AA}$ ). The second feature is a splitter plate which fits into the shock tube at the reflecting wall. The oncoming incident shock is divided and proceeds down two separate channels. One channel is obstructed and the shock is reflected. This pocket of gas serves as the light source ( $I_0$ ). The light passes through a small aperture in the splitter plate, continuing through the gas in the second channel and into the spectrometer through the shutter-valve. The gas in this channel has been processed by the incident shock only, and hence is heated to a significantly lesser degree. The operation of the splitter plate is shown in Fig. 1a, with typical radiation data given in Fig. 1b. for the series of N<sub>2</sub> absorption experiments performed at CAL.<sup>(2, 3, 4)</sup> A test gas mixture of 10% N<sub>2</sub> + 90% Ne was used, giving a reflected-shock temperature of 11,300° K which provided a continuum source of radiation ( $I_0$ ) over the wavelength region of interest.<sup>(8)</sup> The absorbing gas behind the incident shock was at a temperature of 6000° K.

The lower trace in Fig. 1b is from a detector monitoring the total reflected-shock radiation history at a wavelength of about 1300 Å. The upper trace is the recorded signal from one channel of the VUV spectrometer



viewing radiation at  $760 \text{ \AA}$  which has been partially absorbed by the incident shock-heated gas. A comparison of this signal to that obtained with the reflected-shock light source on the spectrometer side of the splitter plate gives the fraction of light transmitted through the heated gas.

This splitter-plate and spectrometer arrangement is being employed for the initial NO absorption experiments. As discussed in the previous Semiannual Report, <sup>(1)</sup> prior to initiating the experimental program, several computations had to be completed in order to define the experimental test conditions. Several criteria must be fulfilled in order to obtain suitable absorption data. For example, the test gas mixture, pressure and incident shock speed must be compatible with: (1) attainment of reflected shock conditions (i. e., temperature) so as to obtain a suitably heated, uniform volume of gas to serve as a continuum light source  $I_0$ , and (2) incident shock conditions of temperature and species density, so as to obtain a measurable range of absorption in the test gas.

Equilibrium shock wave computations <sup>(11)</sup> were initiated for various test gas mixtures and reported in Ref. 1. Based on the previous  $N_2$  experiments, a test gas mixture consisting of 90% neon as the carrier gas, at a total pressure of 2 torr was used in the computations. Neon is used to obtain high reflected shock temperatures and is optically inactive in the wavelength range of interest,  $800 < \lambda < 1100 \text{ \AA}$ . Both incident and reflected shock conditions, over a range of shock strengths, were calculated for the following gas mixtures:

90% Neon + 10% NO

90% Neon + 10% Air (8%  $N_2$  + 2%  $O_2$ )

90% Neon + 5%  $N_2$  + 5%  $O_2$

90% Neon + 2%  $N_2$  + 8%  $O_2$ .

The calculations described in Ref. 1 have been extended and for convenience, the resulting conclusions will be presented herein.

Figure 2 shows the computed incident shock temperature as a function of shock speed. It can be seen that the temperature curves are similar for

various gas mixtures, with temperatures in the range 4500 - 6500° K under consideration for the NO experiments. The corresponding reflected shock temperatures are shown in Fig. 3 for the various gas mixtures. For the incident shock temperatures of interest, the corresponding reflected shock temperatures range from about 8000 - 13,000° K.

Figure 4 presents the NO species concentration behind the incident shock wave. It is the NO concentration, in combination with the wavelength-dependent absorption coefficient that determines the degree of absorption due to NO taking place in the test gas. The calculations presented in Fig. 5 show the ratio of N<sub>2</sub> molecule concentration to that of the NO concentration existing behind the incident shock wave. It can be seen that this ratio reaches a maximum at shock speeds near 13,000 ft/sec.

The combined results of the computations shown in Fig. 2-5 are employed to define the shock velocity and test gas mixture to be used in the initial absorption experiments. Since the N<sub>2</sub> molecule contributes substantially to the absorption process in the wavelength region of interest, it is desirable that the N<sub>2</sub>/NO ratio be kept to a minimum. From Fig. 5, it can be seen that the 10% air-test gas mixture yields ratios greater than 100; thus this mixture cannot be used in the experimental series. As the initial percentage of N<sub>2</sub> is decreased, the resultant N<sub>2</sub>/NO ratio is also decreased, as can be seen from the 2% N<sub>2</sub> - 8% O<sub>2</sub> computation. Here the ratio is over an order of-magnitude lower than the air results. From Fig. 5, then, it can be determined that mixtures other than air are required as the test gas.

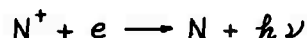
At lower shock velocities, the reflected shock temperature is decreased (see Fig. 3); thus the resultant source radiation, I<sub>0</sub>, is reduced substantially. At higher shock velocities, the reflected shock temperature is increased; however, the absolute value of the NO concentration is substantially decreased (see Fig. 4), which in turn may yield very small values of absorption. The curves in Fig. 4 indicate that the absolute value of NO concentration is relatively insensitive to the initial test gas composition, differing by about a

factor of 2 or 3 for the various mixtures investigated. This can be compared to the  $N_2/NO$  ratio shown in Fig. 5, which was shown to be very sensitive to the initial test gas composition.

On the basis of these computations, it was decided to initiate the series of absorption experiments utilizing the 2%  $N_2$  - 8%  $O_2$  - 90% Neon test gas mixture. Figure 6 shows the incident-shock equilibrium species concentrations for this gas mixture as a function of shock speed. For shock speeds in the range of  $3.8 \times 10^5$  cm/sec, it can be seen that the  $N_2$  concentration is about 20 times that of the NO molecule (i.e., as shown also in Fig. 5). Three other possible absorbing species in the incident-shocked gas are also shown in Fig. 6: the  $O_2$  molecule and the atomic species O and N. However, the NO concentration, for the shock speeds under consideration, is approximately an order of magnitude greater than that of  $O_2$ . But the absorption characteristics of the abundant atomic species must be taken into account. The presence of the N atom at these temperatures for example, leads to absorption below  $850 \text{ \AA}$ , which is the absorption edge of the ground state  $N \rightarrow N^+ + e$  transition. This was observed experimentally during the previous program directed at  $N_2$  absorption coefficients.<sup>(2, 3, 4)</sup> Calculations for the present gas mixture, however, at a shock velocity of  $3.8 \times 10^5$  cm/sec, indicate an absorption of only about 8% for  $\lambda \leq 850 \text{ \AA}$  due to the rather low N atom concentration. Similarly, the presence of the O atom will lead to absorption for wavelengths below  $911 \text{ \AA}$ , which is the absorption edge of the ground state  $O \rightarrow O^+ + e$  transition. Similar calculations indicate approximately 50% absorption for  $\lambda \leq 911 \text{ \AA}$ , due to the large number of O atoms present in the incident-shocked gas. (For these computations, the absorption cross-sections given in Ref. 12 were used). On the basis of these atomic absorption calculations, it can be seen that the molecular NO absorption measurements should be directed toward wavelengths greater than  $911 \text{ \AA}$ .

For the 2%  $N_2$  - 8%  $O_2$  - 90% Ne gas mixture, and a shock velocity of  $3.8 \times 10^5$  cm/sec, the reflected shock temperature is  $11,300^\circ \text{ K}$  (see Fig. 3). The species concentrations in the reflected-shock (light source) region are shown in Fig. 7 as a function of shock speed. The radiation,  $I_o$ ,

from this hot gas is due primarily to the radiative recombination reactions<sup>(8, 9, 10)</sup>



For thermodynamic equilibrium, it is possible to apply photoionization cross-sections to calculate the radiation due to the inverse recombination process,

$$I_\lambda / I_{BB_\lambda} = \epsilon_\lambda = 1 - e^{-L L_0 \left[ \left( \frac{p}{p_0} \right)_O \sigma_{O_\lambda} + \left( \frac{p}{p_0} \right)_N \sigma_{N_\lambda} \right]}$$

where

$I_{BB_\lambda}$  = Blackbody function

$\epsilon_\lambda$  = emissivity

$L_0$  = Loschmidt Number

$l$  = path length

$\sigma_{O_\lambda}, \sigma_{N_\lambda}$  = O atom and N atom absorption cross-sections

Figure 8 shows the O and N atom absorption cross-sections<sup>(12)</sup> at a representative temperature of 11,000° K. The actual values at 11,300° K (the reflected shock temperature) were used to compute the emissivity as a function of wavelength for the reflected shock conditions. The resultant continuum recombination-light source ( $I_O$ ) is shown in Fig. 9 for the test conditions. At wavelengths below 911 Å, the gas approaches blackbody conditions, and becomes optically thin at longer wavelengths.

### II. 1.2 Experimental Results

An initial test series of 30 shock-tube experiments has been completed, of which approximately one-half utilized the splitter plate arrangement. For this preliminary series, the explosively driven plunger which couples the VUV spectrometer to the shock tube was replaced with a LiF window adapter. Thus, wavelengths greater than about 1050 Å were observed during these tests. The primary purpose of the test series was to establish shock-tube performance and radiation characteristics of the various test gas mixtures and to compare these characteristics with measurements from a simple N<sub>2</sub> - Neon test gas. Figure 10 shows a schematic of the experimental arrangement employed for these experiments, with the three endwall

configurations. The primary diagnostic for the reflected shock radiation is a three-channel vacuum-ultraviolet spectrometer. (8, 9, 10) For this present series of experiments, with the LiF window adapter, the grating setting was adjusted such that 1110 Å, 1180 Å and 1625 Å radiation was monitored in first order, with a bandpass of  $\pm 16$  Å. A small mirror inside the spectrometer arm was used to permit a photomultiplier-filter combination to view 5100 Å radiation through the same LiF window. On the opposite side of the shock tube another photomultiplier-filter assembly viewed 2300 Å radiation, and a thin-film heat transfer gauge was used to display the wall temperature rise ( $\Delta T$ ) due to the incident and reflected shock waves (see Fig. 12).

Approximately six feet upstream of the reflecting endwall, several detectors were used to monitor the radiation from the hot gas behind the incident shock wave. Here, two photomultiplier-filter combinations were used to view radiation at 2500 Å and 6600 Å, and an EMR solar-blind PMT was utilized to view radiation in the 1300 Å wavelength range. In addition, a thin-film wall  $\Delta T$  gauge was also displayed to aid in the determination of the incident-shock test time. All of the wavelength intervals chosen for measurements correspond to emitting transitions in the shock heated gas mixture. Spectral intensities from these transitions have previously been recorded and used to monitor the state of the shocked gases. Similarly, the sidewall heat transfer data are used to monitor shock tube operation and repeatability.

The test gas mixtures were admitted to the shock tube through a pumping/loading manifold to an initial pressure of 2 torr. Room temperature hydrogen, at pressures from 650 - 1350 psi, was used as the driver gas. Resultant shock speeds in this test series ranged from approximately 11,500 - 14,000 ft/sec.

Typical reflected shock radiation records are shown in Fig. 11, for several of the test gas mixtures compared in this preliminary test series. The splitter-plate was not installed for these particular tests. For all mixtures, the initial pressure was 2 torr, and the incident shock velocity was nominally 13,500 ft/sec. The data records are obtained from one of the PMT

tubes in the VUV spectrometer centered at  $1110 \text{ \AA}$ , with a bandpass of  $\pm 16 \text{ \AA}$ . Thus, a direct comparison of the VUV radiation at this wavelength can be made for these mixtures, for a constant shock velocity. The reflected shock radiation records (for all wavelengths monitored) are typified by a rise to a plateau-like region after the arrival of the reflected shock wave, a relatively constant value (which indicates the reflected shock test-time) and finally, a sudden increase in intensity as the test-time is ended (due to the arrival of an additional shock wave from the original reflected shock-interface interaction). For this test condition, the reflected-shock test time is seen to be approximately  $130 \text{ \mu sec}$ .

Figure 12 shows data records obtained for three different configurations at the reflecting endwall, all for the same shock speed in the 2%  $\text{N}_2$ /8%  $\text{O}_2$  + 90% Neon test gas mixture. The data records on the right of the figure show the time history of the  $5100 \text{ \AA}$  radiation (as viewed from within the VUV spectrometer, see Fig. 10) for the three configurations. It can be seen that the time-history of the reflected shock radiation is typical of the data shown in the previous figure, with the test time indicated by the duration of the plateau region. Also shown on these records is the output from a thin-film wall temperature gauge located near the  $2300 \text{ \AA}$  viewing port (see Fig. 10). The upper and lower records show the gauge output for: (a) a sudden rise to a short plateau region which corresponds to the incident shocked gas, and (b) the subsequent parabolic increase in temperature which is characteristic of the heat transfer due to the reflected shock gas. These data can be compared with the trace shown in the middle record, which shows only the constant-temperature plateau typical of incident-shocked gas only; this shows the passage of the incident shock along one side of the splitter plate. The rise in temperature after a period of about  $200 \text{ \mu sec}$  shows the extent of the incident-shocked slug of gas. Superimposed on this record is the  $5100 \text{ \AA}$  radiation trace from the reflected pocket on the opposite side of the splitter plate. It can be seen that the reflected-shock test time (source of  $I_0$  radiation) is properly timed with the passage of the incident-shocked gas for the absorption measurements.

The three data records on the left of Fig. 12 show the measured 1110 Å radiation for the three test configurations. The two upper records, in which the spectrometer viewed the reflected gas pocket directly, show the typical time history, as shown in Fig. 11, for example. The lower trace shows the 1110 Å time history when the reflected gas pocket is on the opposite side of the shock tube and is viewed through the incident-shocked gas. For this particular gas mixture, the second peak in radiation (which indicates the end of the test time) was not observed at this wavelength, although it is clearly seen by the detector viewing 5100 Å, shown in the record to the right of the figure. (It should be noted that for similar tests in this series, using a 10% N<sub>2</sub> + 90% Neon mixture, the second radiation peak was observed at the VUV wavelengths for the same splitter plate configuration). The records shown in Fig. 12 indicate that for the 2% N<sub>2</sub>/8% O<sub>2</sub> gas mixture, sufficient absorption occurred at the VUV wavelengths to prevent this second peak from being observed.

Previous measurements<sup>(2, 3, 4)</sup> and calculations indicate that the incident-shocked gas should be transparent at the wavelengths investigated during this test series (1110 Å, 1180 Å, 1625 Å). However the splitter-plate data obtained for both the 2% N<sub>2</sub>/8% O<sub>2</sub> and 10% N<sub>2</sub> mixture indicate a substantially lower signal when the reflected pocket is on the opposite side of the shock tube, i. e.,  $I/I_0 \approx .25$ . Earlier experiments<sup>(8, 9, 10)</sup> indicated that there could be substantial absorption in the boundary layer near the explosively driven plunger entrance, if sufficient care were not taken to pump away the boundary layer. It will be determined if this is the cause of the reduced signals during the next series of tests in which the explosively driven plunger will be employed.

Comparisons of calculated radiation and experimental measurements were obtained for two reflected shock temperatures for the 2% N<sub>2</sub>/8% O<sub>2</sub> test mixture at 2 torr.

The continuum emissivity values at the three experimental wavelengths were computed (see Section II. 1. 1) and used with the appropriate blackbody curves to obtain the predicted radiation for the two temperatures (similar to Fig. 9.). The ratios of the continuum intensities are given as:

Wavelength, Å	Ratio $\frac{I_{12,500^\circ \text{ K}}}{I_{10,950^\circ \text{ K}}}$ calculated	Ratio $\frac{I_{12,500^\circ \text{ K}}}{I_{10,950^\circ \text{ K}}}$ measured
1110 Å	4.65	4.5
1180 Å	13.5	5.5
1625 Å	10.7	8

For the 1110 Å and 1625 Å wavelengths, the calculated and measured ratios are in reasonable agreement. However, at 1180 Å, the ratios differ by about a factor of two (i. e., the measured results indicate a much smaller change in radiation with a change in temperature). The data of Ref. 12 show several extremely strong lines, due to transitions from various states of the N atom, within the bandpass of the detector. These lines are located at 1171, 1181 and 1190 Å. It is felt that the experimental data at this wavelength setting includes contributions from these lines thus the ratio will not reflect only the calculated change in the continuum background. This will be pursued during the next series of experiments.

## II. 2 Nonequilibrium Overshoot Radiation Measurements

### II. 2. 1 Calculations

For the 2% N<sub>2</sub>/8% O<sub>2</sub> test gas, a nonequilibrium shock calculation was obtained to investigate the relaxation processes behind the incident shock wave. The normal shock program developed at CAL<sup>(13)</sup> was used to compute the finite-rate chemical reactions and gasdynamic behavior behind a shock traveling at 3.75 x 10<sup>5</sup> cm/sec (12,300 ft/sec) into 2 torr pressure



of the gas mixture. Figures 13 and 14 show the resultant temperature and species concentration profiles near the shock front (i. e., for the first 22  $\mu\text{sec}$  of measured laboratory time). The immediate post-shock temperature (assuming vibrational equilibrium of the  $\text{N}_2$  and  $\text{O}_2$ ) is  $6560^\circ\text{K}$ , and rapidly decays toward the final equilibrium value of approximately  $4760^\circ\text{K}$ , see Fig. 2. The species concentrations are shown in Fig. 14, where the time involved to establish near equilibrium conditions is more clearly observed. There is an initial overshoot in the  $\text{NO}$  concentration (a maximum near 12  $\mu\text{sec}$ ) and a decay toward the final equilibrium value. Fifty microseconds after passage of the shock wave, the temperature is within 1% of its final value and the  $\text{NO}$  concentration is within about 20% of its final value. This relaxation time can be compared with the total incident-shock slug duration of about 200  $\mu\text{secs}$ , as indicated by the  $\Delta T$  record in Fig. 12, and discussed in Section II. 1. 2.

### II. 2. 2 Experimental Results

In addition to the reflected shock measurements discussed earlier, additional measurements of the nonequilibrium radiation overshoot behind the incident shock were also obtained during the test series, utilizing the instrumentation indicated in Fig. 10. Typical data for several of the test gas mixtures is shown in Fig. 15., for two different shock speeds. In general, the radiation data shown is typified by a sudden increase upon passage of the incident shock past the viewing port. The radiation then reaches an overshoot maximum close to the shock front and subsequently decays toward the final equilibrium value.

The measurements show substantial radiation at  $6600 \text{ \AA}$  for only the 10%  $\text{N}_2$  test mixture, (Fig. 15a); this radiation arises from the  $\text{N}_2(1+)$  band system. Differences in the radiation time history for the  $1300 \text{ \AA}$  wavelength are readily observed for the different test gas mixtures shown in the figure. For 10%  $\text{N}_2$ , there is a well defined overshoot occurring about 50  $\mu\text{sec}$  after shock passage (Fig. 15a). However, for the 10%  $\text{NO}$  mixture (Fig. 15b), the data indicate a long plateau-like region, with no clearly definable nonequilibrium overshoot. This is similar to the results obtained

for the 2% N<sub>2</sub>/8% O<sub>2</sub> gas mixture (Fig. 15a).

For all the gas mixtures, the 2500 Å measurements showed a clearly defined overshoot maximum occurring near the shock front. The data are shown at two different oscilloscope sweep speeds, the larger record having expanded the time near the shock front. For the 10% N<sub>2</sub> mixture, this radiation, which arises from the N<sub>2</sub>(4+) band system, does not show the rapid decay apparent in the other records, but rather, a slow decline toward the equilibrium level. When NO is present behind the shock wave, the peak overshoot value at this wavelength increases substantially. This can be seen in Fig. 15a when comparing the 2500 Å data for the same nominal shock velocity. For the 2% N<sub>2</sub>/8% O<sub>2</sub> test gas, NO is formed behind the shock wave (similar to the computations shown in Fig. 14). The peak radiation value is approximately 10 times greater for the N<sub>2</sub>/O<sub>2</sub> mixture than for the pure nitrogen case. The radiation at this wavelength is dominated by the NO (γ) system when the NO molecule is present. This is also shown in Fig. 15b for a slower shock velocity. When NO is present initially in the test mixture (i. e., the 10% NO gas) the peak value is approximately 8 times the value of that measured when NO is formed from the initial N<sub>2</sub>/O<sub>2</sub> species.

The incident shock records shown on the right side of Fig. 15b can be compared with the calculations shown in Figs. 13 and 14 for the same nominal shock speed. From the upper record, it is seen that the peak 2500 Å value is reached about 5 μsec after shock passage, when the temperature has already decreased by about 1500° K. This is also near the computed time for peak NO concentration. The lower data record in Fig. 15b, with a time sweep of 20 μsec/div, shows the complete 2500 Å time history for the duration of the incident-shocked test gas. It can be seen that this nonequilibrium overshoot occurs extremely early in the approximately 160 μsec of test time. This record can be compared to the sidewall ΔT record which also shows the duration of the test gas slug; the increase in ΔT near the end of the record indicates the end of the incident shock test time at this station in the shock tube. By comparing this record with the middle record shown in Fig. 12, it can be seen that the splitter-plate VUV absorption measurements are obtained when the incident-shocked gas has substantially obtained its final equilibrium level.

### III. CURRENT STATUS AND FUTURE PLANS

The preliminary test series for various test gas mixtures has been completed. Vacuum-ultraviolet radiation measurements have been obtained for the 1100 Å - 1650 Å wavelength interval, and the final test gas mixture and shock velocity to be used for NO measurements have been determined from these tests. The major emphasis for the next six weeks will be directed toward the final NO absorption and nonequilibrium radiation measurements. A test gas mixture of 2% N<sub>2</sub>/8% O<sub>2</sub> + 90% Neon will be used, at a nominal incident-shock velocity of 12,500 ft/sec. VUV measurements will be obtained in the wavelength interval 900 - 1200 Å, using the explosively driven plunger assembly to couple the spectrometer to the shock tube.

### ACKNOWLEDGEMENT

The work reported herein was primarily performed by Dr. P. V. Marrone and Mr. J. E. Stratton.

## REFERENCES

1. Wurster, W.H.: Experimental Studies of Photoionization Processes in Air; Semiannual Technical Report for Period 1 May 1971 to 1 November 1971. Cornell Aeronautical Laboratory Report No. AI-3107-A-1, November 1971.
2. Marrone, P.V. and Wurster, W.H.: Reentry Precursor Plasma-Determination of the Vacuum Ultraviolet Photoionizing Radiative Flux. Paper Presented at the 4th Entry Plasma Sheath Symposium. NASA Langley Research Center. October 13-15, 1970.
3. Precursor Ionization From Blunt Body Shock Waves: Annual Technical Report. Prepared by W.H. Wurster, Cornell Aeronautical Laboratory Report No. AF-2581-A-2, July 1970.
4. Edwards, K.R., Marrone, P.V., Olson, G.E. and Wurster, W.H. The Photoionized Precursor Plasma and Its Effect on Blunt Body Radar Observables (U). Presented at the AIAA Joint Strategic Missile Sciences Meeting. U.S. Naval Academy, Annapolis, Maryland. 10-12 May, 1971 (SECRET).
5. Watanabe, K., Matsunga, F.M. and Sakai, H.: Absorption Coefficient and Photoionization Yield of NO in the Region 580-1350 Å. Applied Optics, Vol. 6, No. 3. March 1967. pp. 391-396.
6. Cook, G.R. and Ching, B.K.: Absorption, Photoionization, and Fluorescence of Some Gases of Importance in the Study of the Upper Atmosphere. Aerospace Corporation Report No. TDR-469(9260-01)-4. January 1965.
7. Watanabe, K. Marmo, F.F. and Inn, E.C.Y.: Photoionization Cross Section of Nitric Oxide. Physical Review, Vol. 91, 1953, p. 1155.
8. Marrone, P.V., Wurster, W.H. and Stratton, J.E.: Shock-Tube Studies of  $N^+$  and  $O^+$  Recombination Radiation in the Vacuum Ultraviolet. Cornell Aeronautical Laboratory Report No. AG-1729-A-7. June 1968.
9. Marrone, P.V. and Stratton, J.E.: Vacuum Ultraviolet  $C^+$  Recombination Radiation from Shock Heated CO/Ne Mixtures. Cornell Aeronautical Laboratory Report No. RH-2786-A-1. March 1970.
10. Marrone, P.V. and Wurster, W.H.: Measurement of Atomic Nitrogen and Carbon Photoionization Cross Sections Using Shock Tube Vacuum Ultraviolet Spectroscopy. JQSRT, Vol. 11, No. 4. April 1971. pp. 327-349.

11. Williams, M.J. and Garr, L.J.: A Description of the CAL Equilibrium Normal Shock Program. Cornell Aeronautical Laboratory Internal Memorandum, September, 1966.
12. Willson, K.H. and Nicolet, W.E.: Spectral Absorption Coefficients of Carbon, Nitrogen, and Oxygen Atoms. JQSRT. Vol. 7, No. 6. November/December 1967 (pp. 891-943).
13. Marrone, P.V.: Inviscid, Nonequilibrium Flow Behind Bow and Normal Shock Waves, Part I. General Analysis and Numerical Examples. Cornell Aeronautical Laboratory Report No. QM-1626-A-12(I). May 1963.

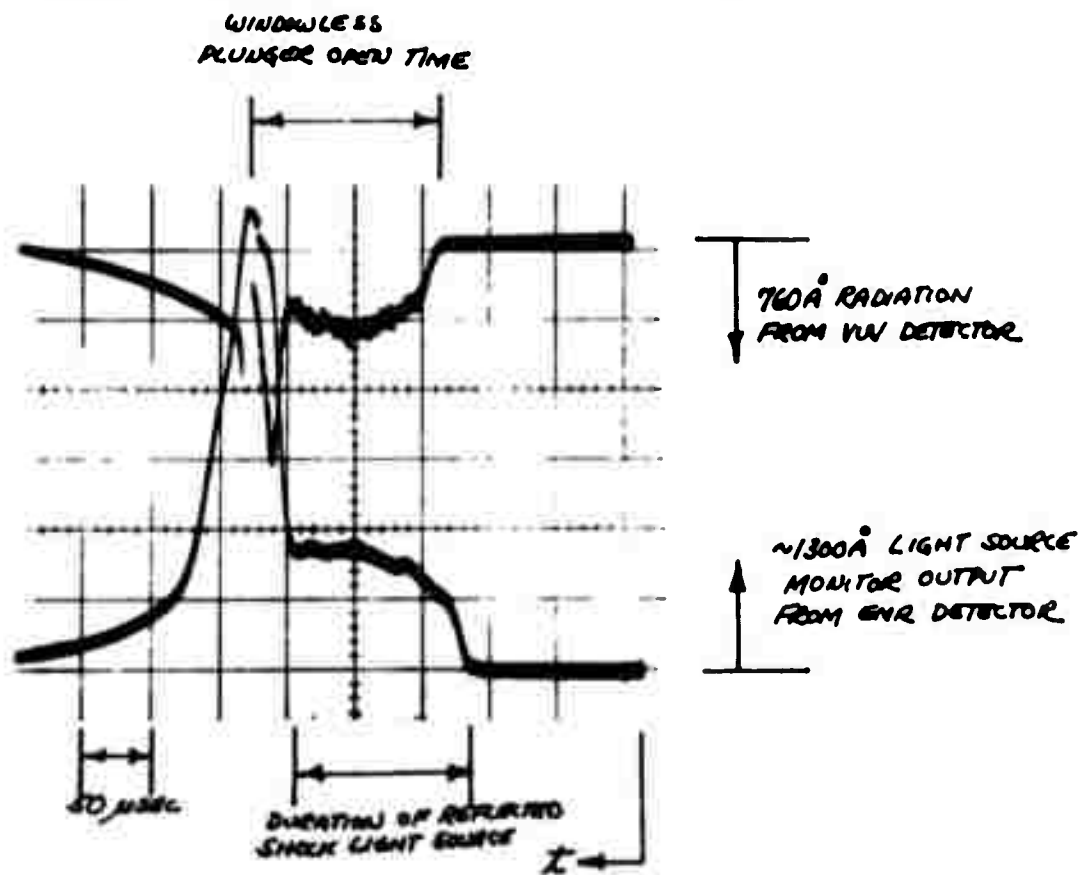
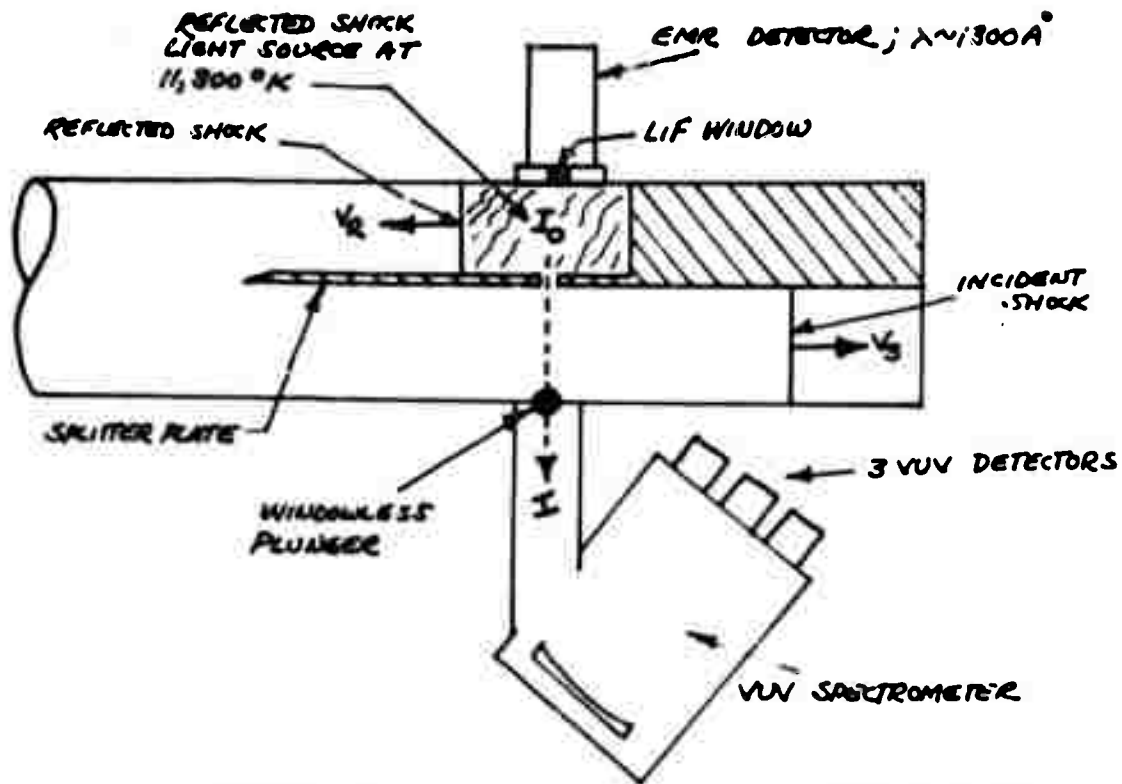
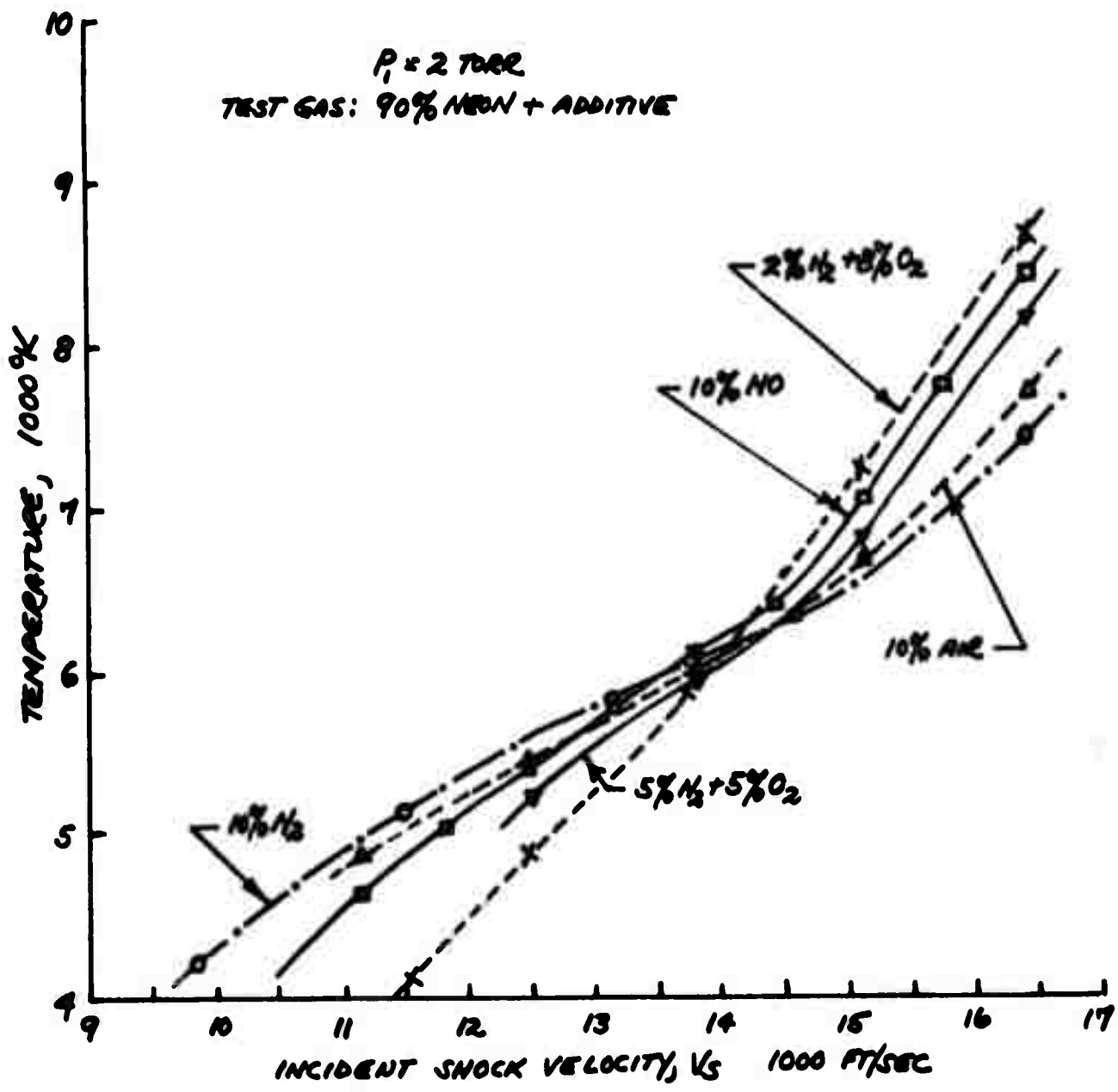
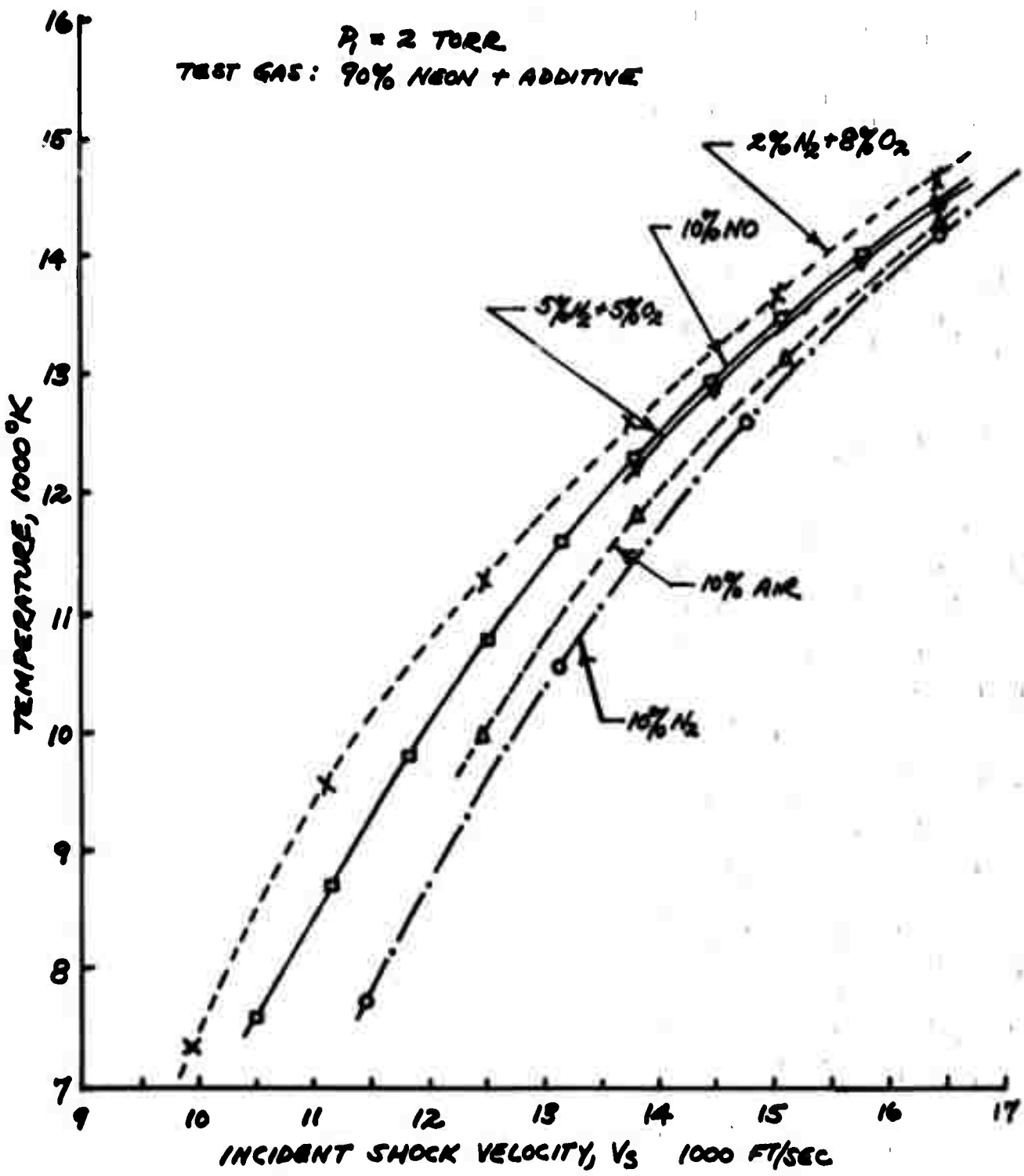


FIG. 1 (a) VUV EXPERIMENT (b) TYPICAL RADIATION DATA



**FIG. 2** CALCULATED EQUILIBRIUM TEMPERATURE  
 BEHIND INCIDENT SHOCK WAVE



**FIG. 3** CALCULATED EQUILIBRIUM TEMPERATURE BEHIND REFLECTED SHOCK WAVE



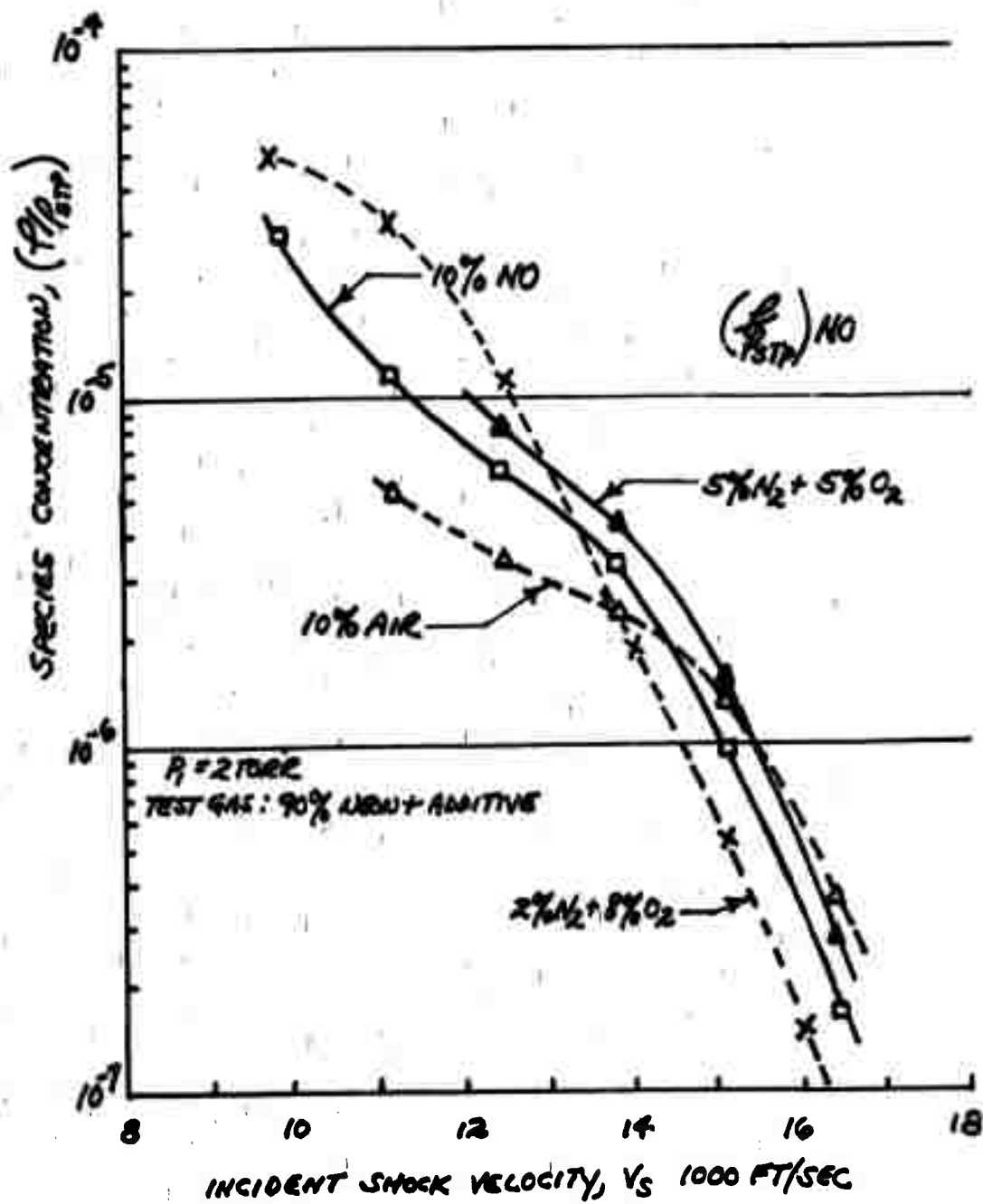


FIG. 4 CALCULATED  $[NO]$  CONCENTRATION  
 BEHIND INCIDENT SHOCK WAVE

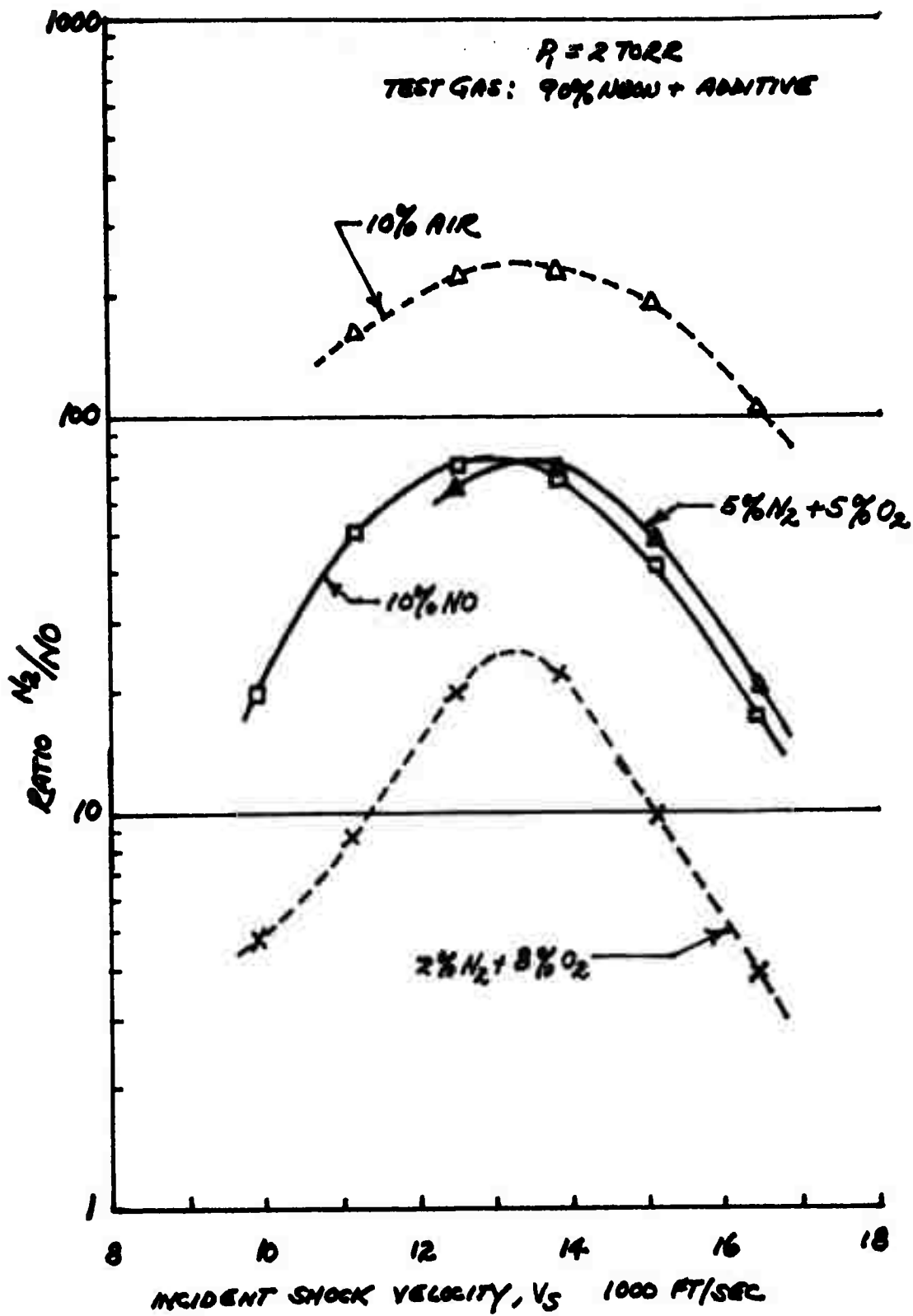


FIG. 5 CALCULATED RATIO OF  $N_2/NO$  CONCENTRATION  
BEHIND INCIDENT SHOCK WAVE

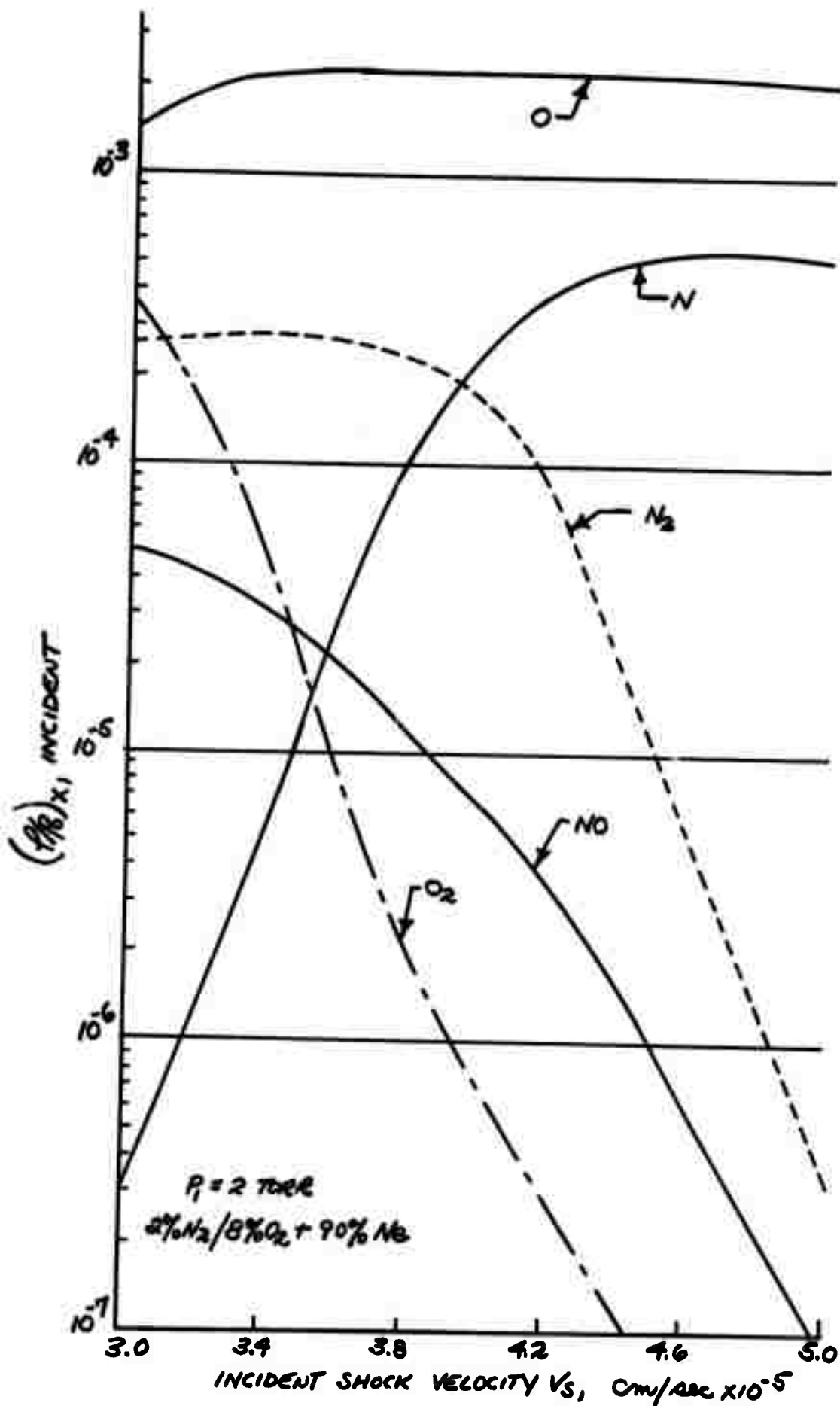


FIG. 6 CALCULATED SPECIES CONCENTRATIONS BEHIND INCIDENT SHOCK WAVE

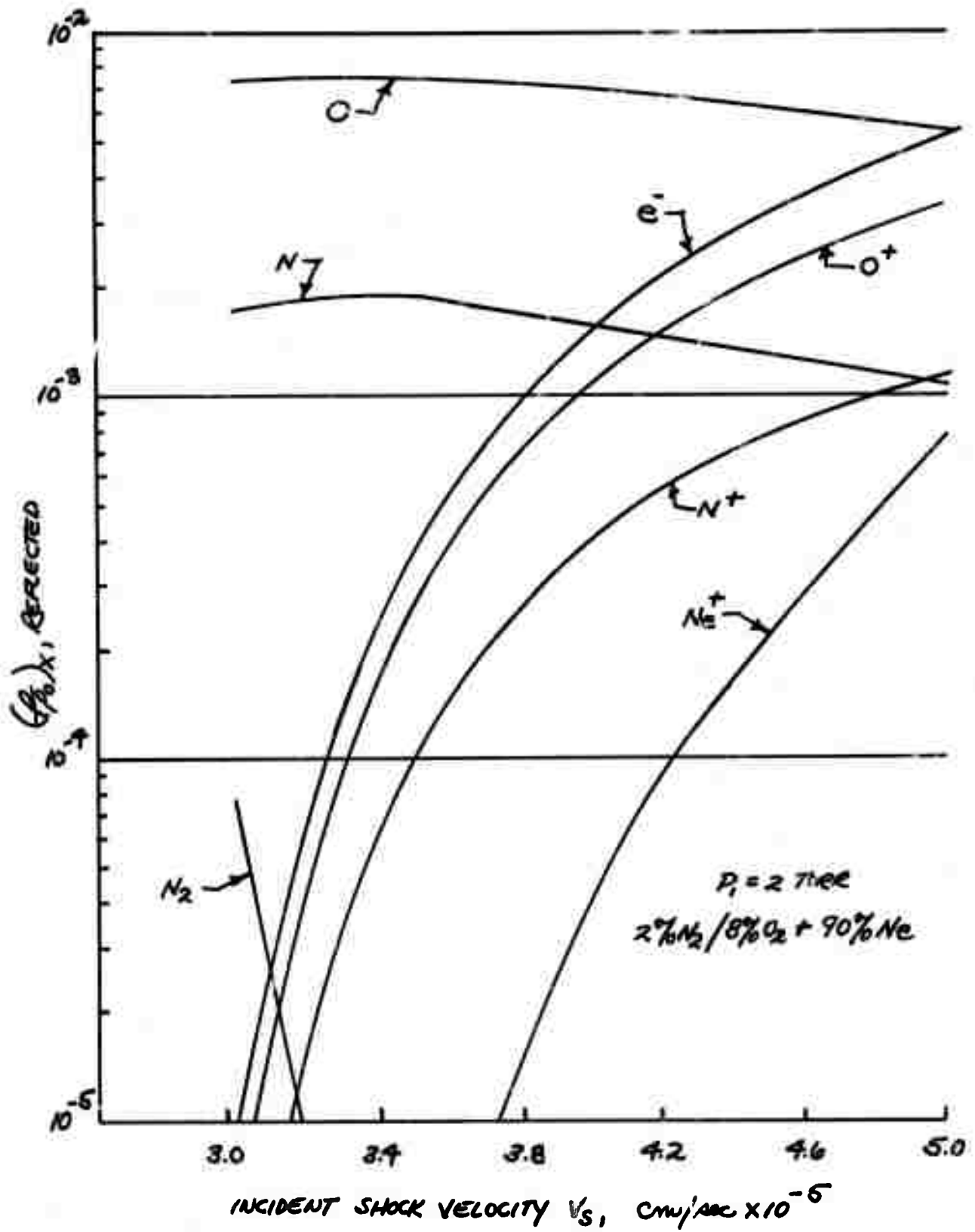


FIG. 7 CALCULATED SPECIES CONCENTRATIONS BEHIND REFLECTED SHOCK WAVE

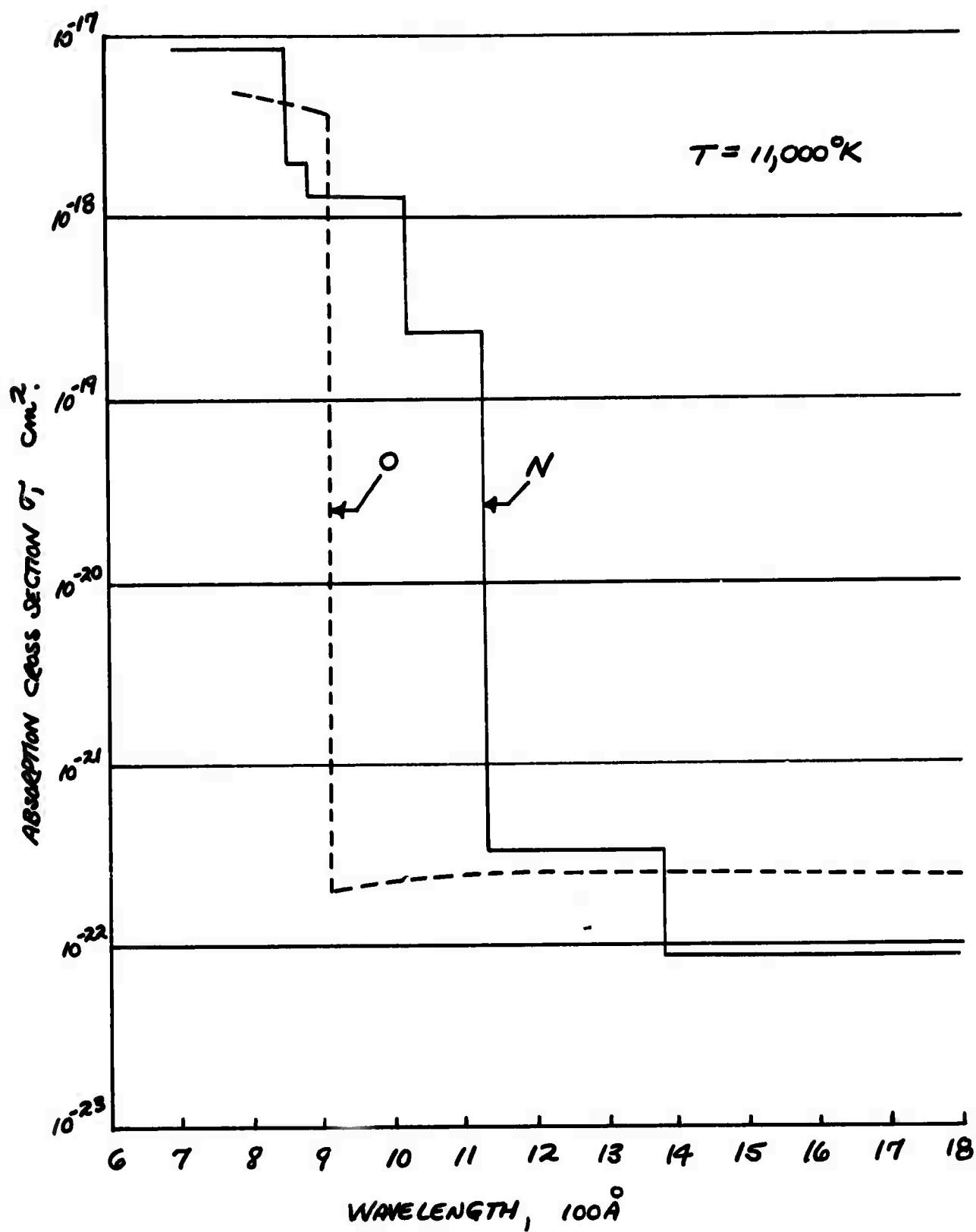


FIG. 8 ABSORPTION CROSS-SECTIONS (FROM REF. 12)

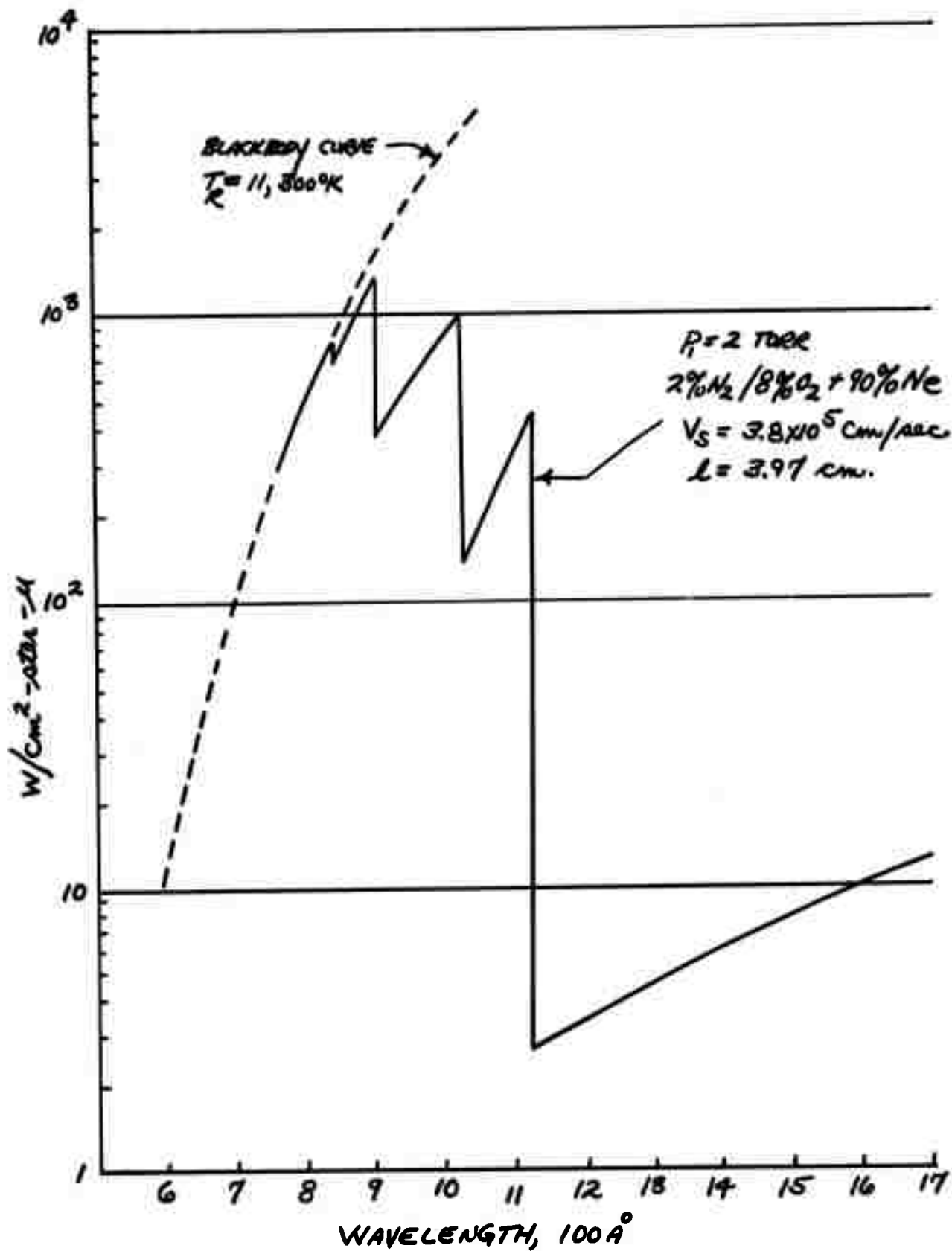


FIG. 9 CALCULATED CONTINUUM RADIATION BEHIND REFLECTED SHOCK WAVE

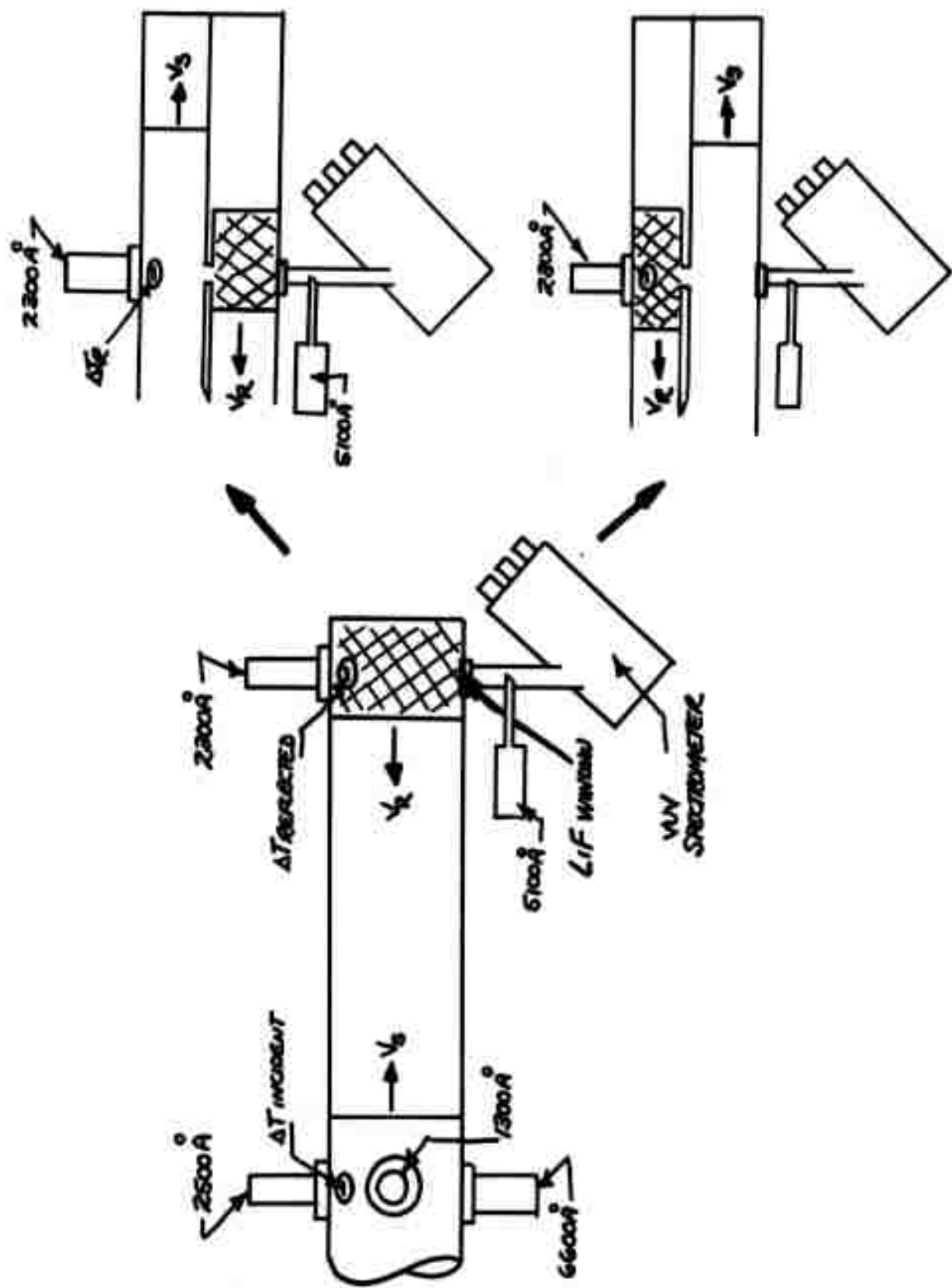
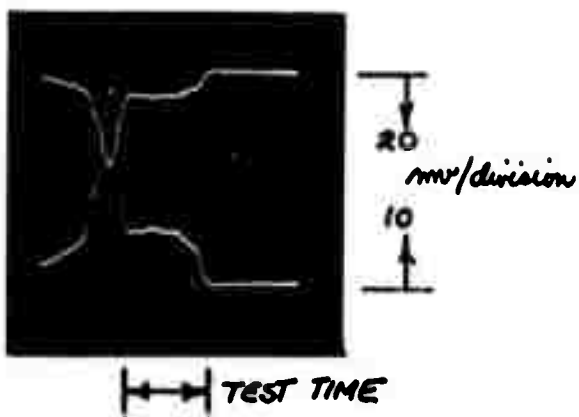
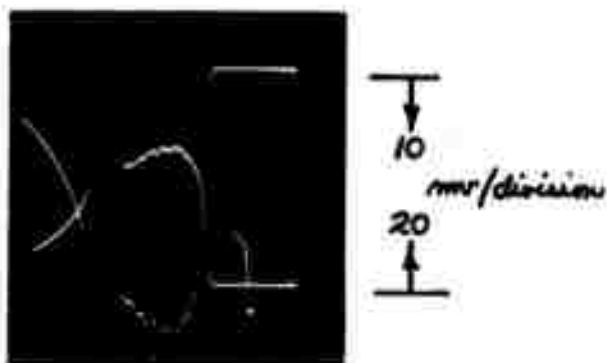


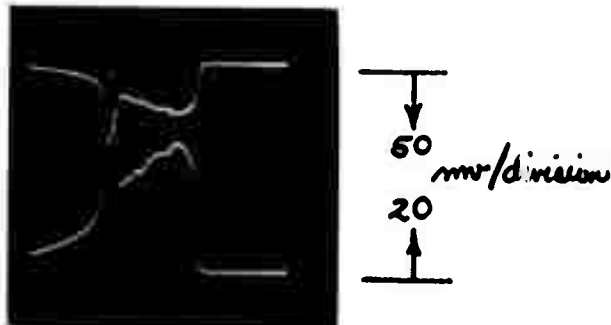
FIG. 10 SCHEMATIC OF EXPERIMENTAL SHOCK-TUBE CONFIGURATIONS



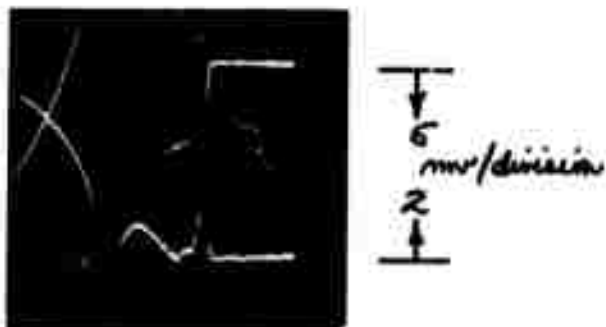
10% N<sub>2</sub> + 90% Ne  
 $T_R \approx 11,100^\circ\text{K}$



10% NO + 90% Ne  
 $T_R \approx 12,000^\circ\text{K}$



5% CO + 95% Ne  
 $T_R \approx 12,400^\circ\text{K}$



2% N<sub>2</sub>/8% O<sub>2</sub> + 90% Ne  
 $T_R \approx 12,400^\circ\text{K}$

TIME ← 50 μsec/division

FIG. 11 REFLECTED SHOCK RADIATION DATA ( $\lambda = 1110\text{\AA}$ ,  $\Delta\lambda = 32\text{\AA}$ );  
 $P_i = 2 \text{ TORR}$ ,  $V_s \approx 13,500 \text{ ft/sec}$ .



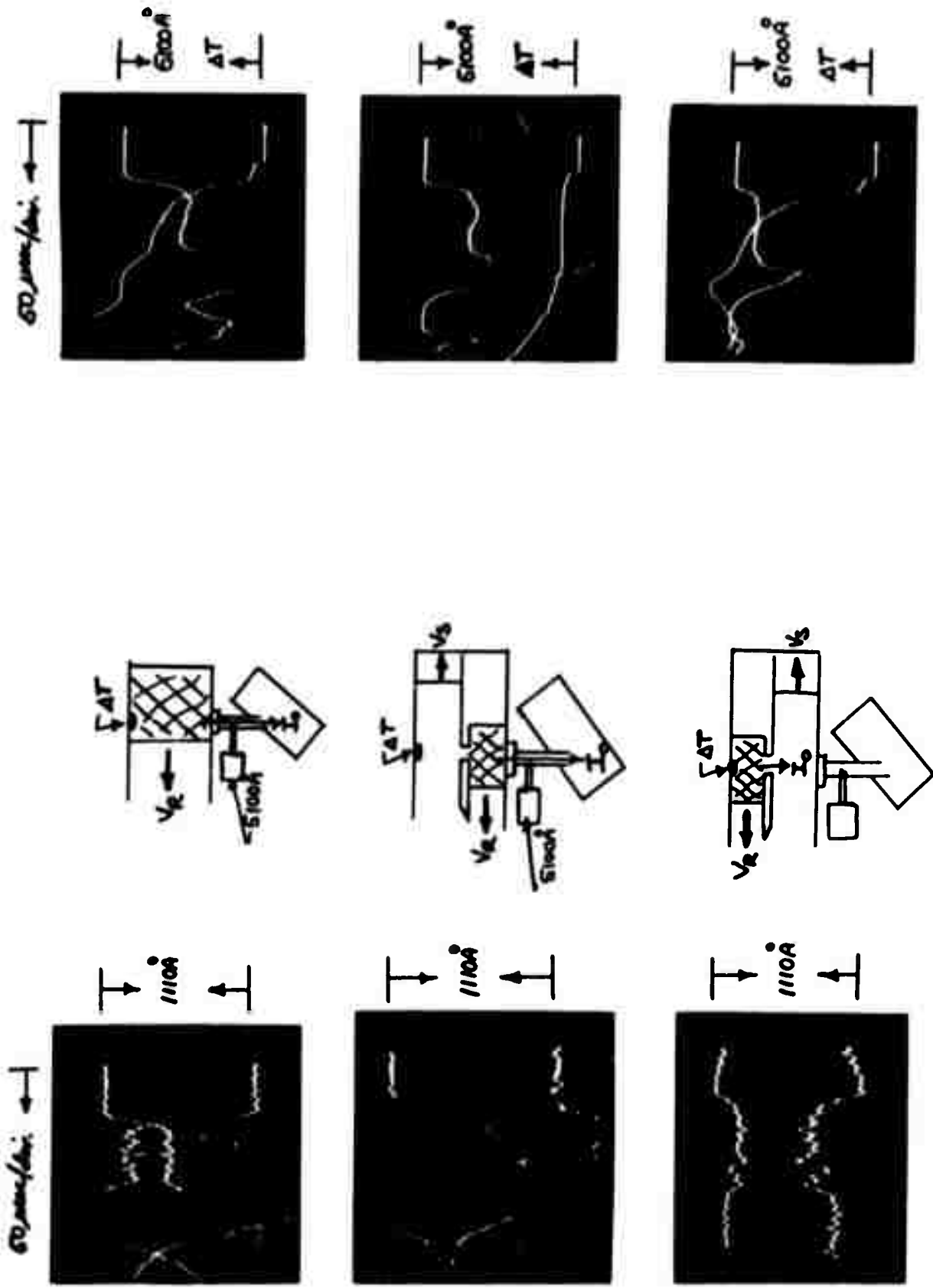


FIG. 12 REFLECTED SHOCK MEASUREMENTS: 2%  $N_2$ /8%  $O_2$  + 90% Ne  
 $P_1 = 2$  Torr,  $V_s = 12,500$  ft/sec,  $T_R \approx 11,300$  K

$P_1 = 2 \text{ TORR}$   
 $2\% \text{ N}_2 / 8\% \text{ O}_2 + 90\% \text{ He}$   
 $V_S = 2.75 \times 10^5 \text{ cm/sec}$

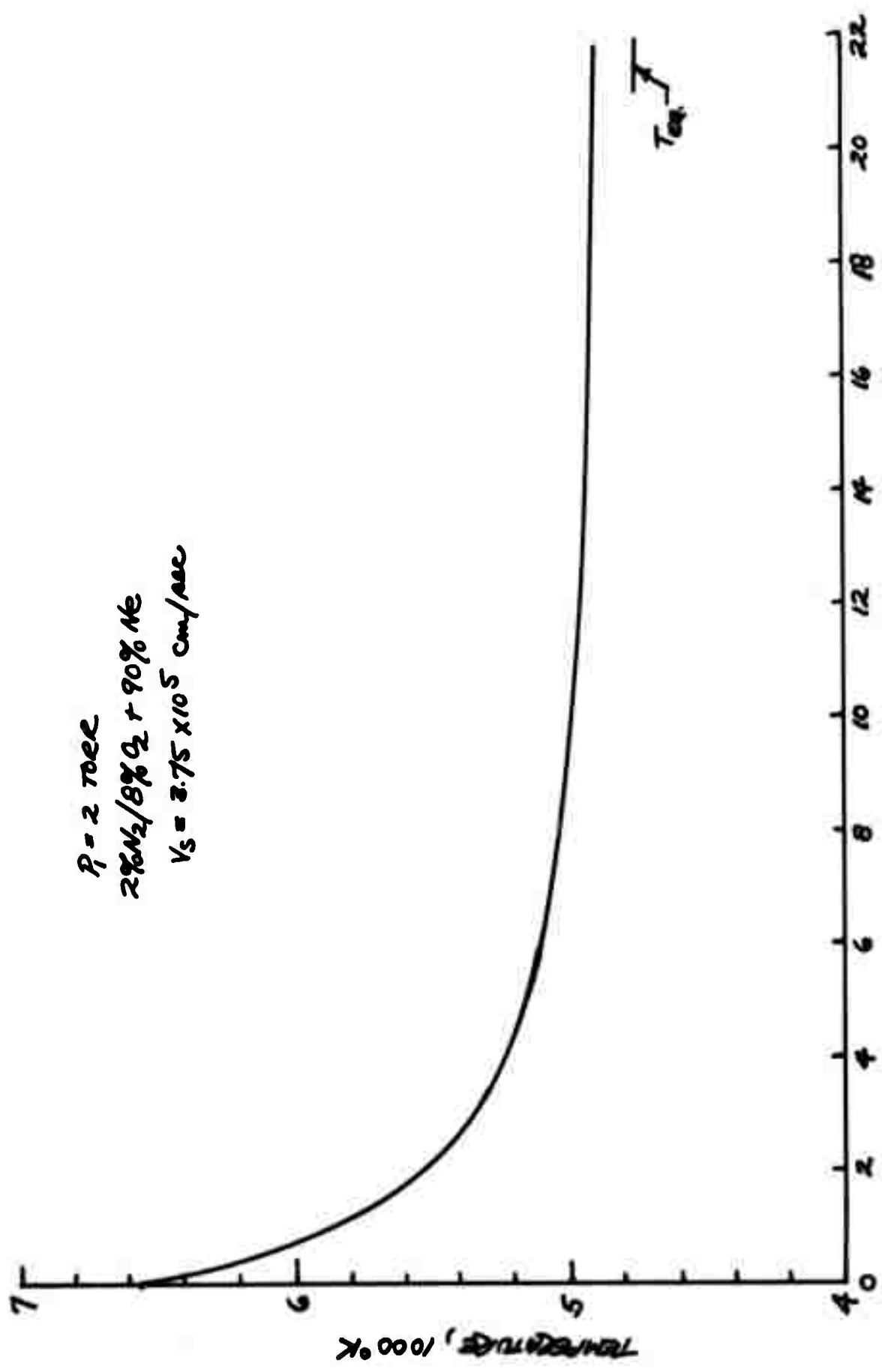


FIG. 13 CALCULATED TEMPERATURE DISTRIBUTION BEHIND  
 INCIDENT SHOCK WAVE

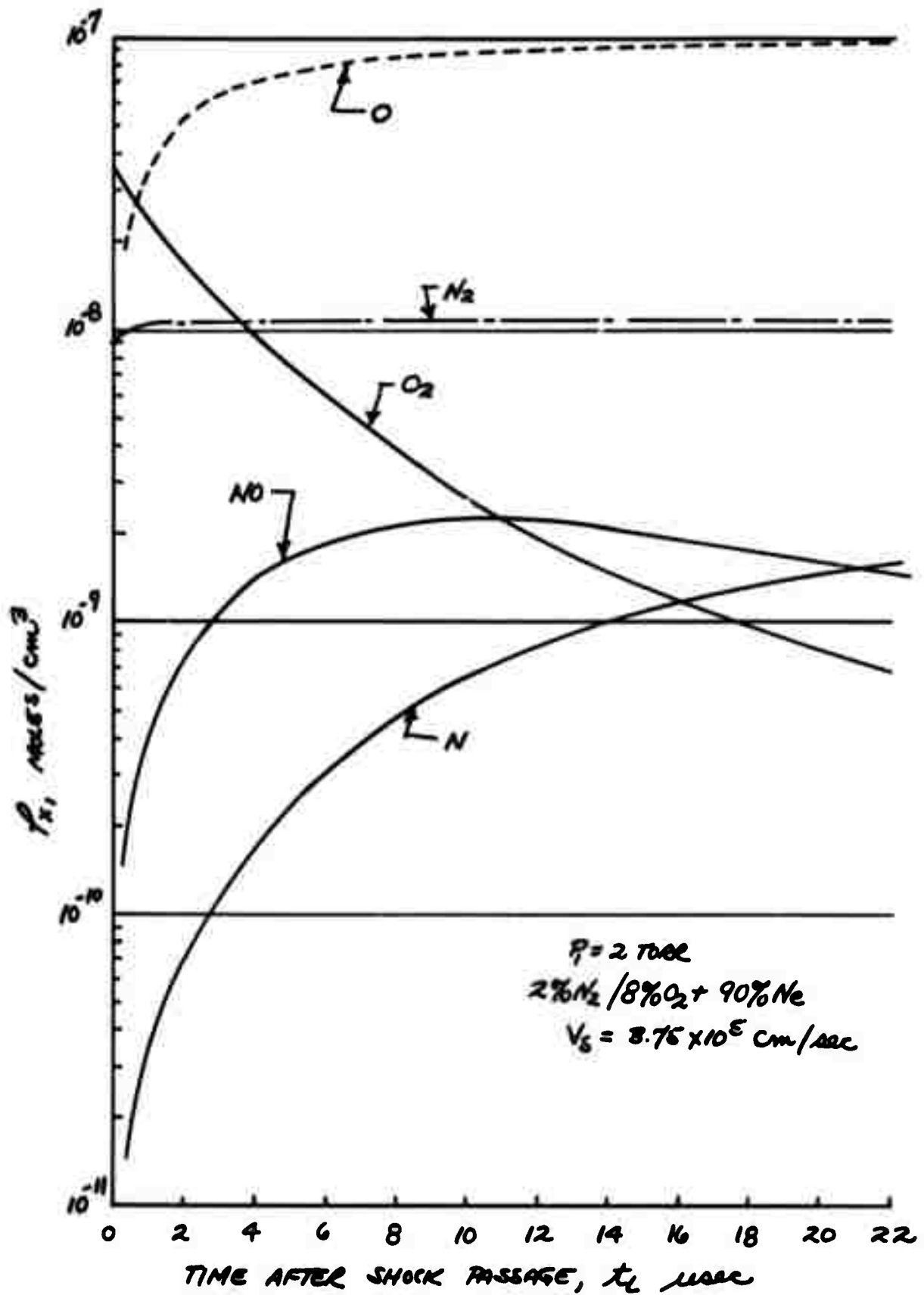


FIG. 14 CALCULATED SPECIES DISTRIBUTION BEHIND INCIDENT SHOCK WAVE



100 mm/div.  
2500 Å

→ 2 μsec/div.



1300 Å  
1 mm/div.  
5 mm/div.  
6600 Å

→ 20 μsec/div.



ΔT  
100 mm/div.  
2500 Å

$P_1 = 2 \text{ Torr}$   
10%  $N_2$  + 90%  $Ne$   
 $V_s = 13,700 \text{ ft/sec.}$



500 mm/div.  
2500 Å

→ 2 μsec/div.



1300 Å  
1 mm/div.  
1 mm/div.  
6600 Å

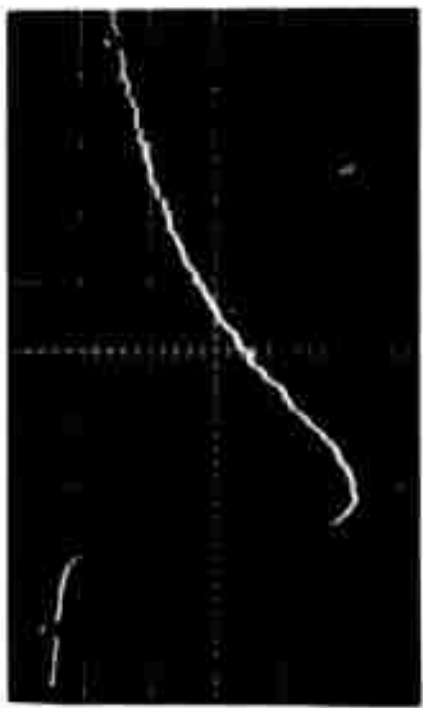
→ 20 μsec/div.



ΔT  
500 mm/div.  
2500 Å

$P_1 = 2 \text{ Torr}$   
29%  $N_2$  / 88%  $O_2$  + 90%  $Ne$   
 $V_s = 13,900 \text{ ft/sec.}$

FIG. 15 a. TYPICAL INCIDENT SHOCK DATA



1000 mV/div  
2500 A

2 μsec/div



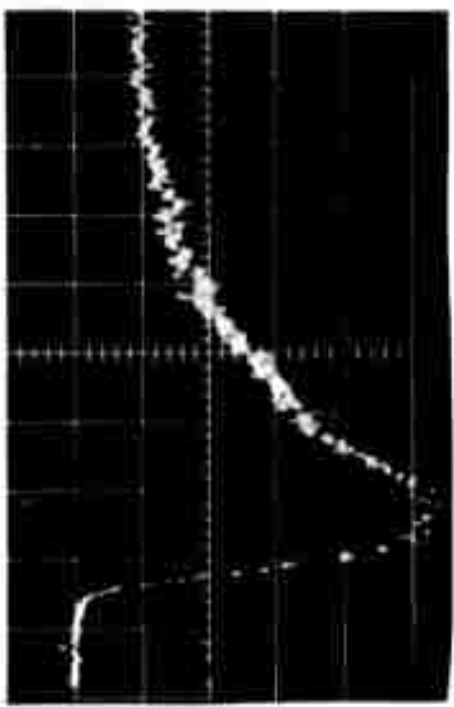
1000 A  
1 mV/div  
6600 A

20 μsec/div



ΔT  
2000 mV/div  
2500 A

$A = 2.7 \text{ Mbar}$   
 $10\% \text{ NO} + 90\% \text{ Ar}$   
 $V_s = 12,700 \text{ ft/sec}$



100 mV/div  
2500 A

2 μsec/div



1000 A  
1 mV/div  
6600 A

20 μsec/div



ΔT  
100 mV/div  
2500 A

$A = 2.7 \text{ Mbar}$   
 $2\% \text{ H}_2 / 8\% \text{ O}_2 + 90\% \text{ Ar}$   
 $V_s = 12,700 \text{ ft/sec}$

FIG. 15 b. TYPICAL INCIDENT SHOCK DATA